Validation of polyurethane foam models in Alfonso™: Uniaxial compression

Non-Confidential Internal Technical Whitepaper – 31 March 2023

Experiments and Analysis: Janice Oentaryo, PhD; Rezaul Tharim; Sloan Kulper, PhD; and Erica Ueda Boles, PhD
Visualizations: Abbas Alvi and Eka Tjong

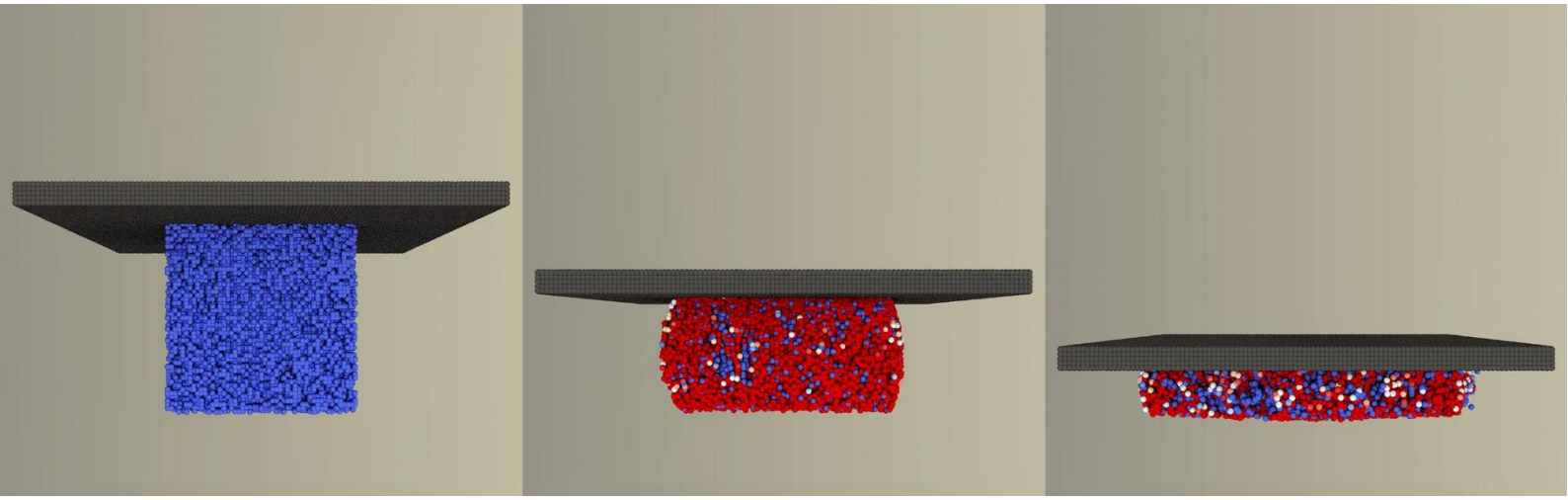

Abstract

Computational models of the uniaxial compression of several common grades of solid rigid polyurethane foam were generated using the particle-based simulation system *Alfonso*, and validation was performed via correlation with experimental data. Six cubes (10 mm on a side) were prepared for each of four grades of solid rigid polyurethane foam (10, 15, 20, and 40 PCF per the ASTM F1839-08-2021 standard). These cubes were then compressed uniaxially at 2.5 mm/min to 10-15% of their original height. Particle-based models of equivalent porosity for each foam grade were generated in *Alfonso* at a resolution of 200 µm/particle, and then compressed uniaxially. The concordance correlation coefficient between the force-displacement curves of experimental and simulated pairs was 0.99, 0.99, 0.98, and 0.87 for 10, 15, 20, and 40 PCF foam, respectively. Experimental and simulated pairs likewise produced similar qualitative patterns of damage during compression. *Alfonso* can generate highly accurate models of PU foam compression and failure, especially for low and medium-density foam grades.

Background and objectives

Solid rigid polyurethane (PU) foams have been extensively and widely used as standard test materials in orthopaedic biomechanical experiments to mimic human cancellous bones [1], [2]. Due to the polymerization of PU monomers, the reaction of water and isocyanate groups generates carbon dioxide, which results in the closed cell structure of PU foam. Although this differentiates PU foam from the open porosity of cancellous bone, PU foam still shares comparable macrostructure with cancellous bone, and it excels in its uniformity and consistency of material properties that are often highly variable in cadaveric bones. Existing literature studies have reported how PU foams mimic the mechanical properties of cancellous bone [1]–[4]. In monotonic compression, PU foams also exhibited similar stress-strain curves as cancellous and trabecular bone [5].

Leveraging the concept of mesh-free modelling to represent material damage in other industries, *Alfonso* is the first tool of its kind in orthopaedics to use a mesh-free modelling method to simulate an implant in bone or polyurethane foam as discrete particles. Particle-based methods excel at representing material failure phenomena such as the cracking and crushing of bone or polyurethane foam that occurs during implant testing, which are generally not practical to simulate using mesh-based methods (e.g., finite element analysis or FEA). *Alfonso* uses point-based input files of the 3D models of the implant and polyurethane foam blocks per ASTM F1839-08(2021) of any foam grade or density based on the customer's request. Most of the standard methods testing the performance of medical bone screws, spinal spacers, and joint replacement implants require the use of polyurethane foam blocks of a certain grade and density per ASTM F1839 as a suitable bone surrogate model. To test the validity of *Alfonso's* foam models, we compare physical and simulated uniaxial foam compression validation tests on different PU foam grades (10, 15, 20 and 40 PCF) with material properties based on the ASTM F1839-08(2021) standard.

Materials and methods

Preparation of physical polyurethane foam specimens

Physical solid rigid polyurethane foam specimens (n=6 each of 10, 15, 20, and 40 PCF densities) were prepared by cutting the manufacturer-supplied block (130x18x40 mm) into cubes measuring 10 mm on a side. The direction of foam rise was noted to ensure that foam rise always aligned with the axis of compression. Material properties for the PU foam grades tested are listed in Table 1.

Preparation of simulated polyurethane foam models

Simulated solid rigid polyurethane foam specimens were prepared by generating particle-based models of four foam grades (10, 15, 20, and 40 PCF) in *Alfonso*, using micro-CT scans of the corresponding physical materials as reference. These simulated foam models contained a randomized distribution of pores designed to mimic the generally isotropic structure of the physical material. The volume fraction of each simulated foam grade was measured and found to be approximately equal that of its real-world counterpart (see Table 1). All foam models were generated at a resolution of 200 μm (i.e., the minimum effective distance at which particle are considered "neighbors," and interaction begins). This resolution was selected to balance accuracy with computational time, based on the prior experience of the engineering team. Bonds were formed between initially-neighboring foam particles to create porous geometry analogous to the physical specimens (see "Notes on the particle-based methods in *Alfonso*" below for further detail).

A review of the literature suggests that coarse model resolutions lead to stiffening when simulating porous compressible solids like bone or foam [6], though the effect size appears to decrease with porosity. To compensate for this effect, an iterative process was used to determine the appropriate material properties required for each simulated foam model to converge with the properties of the physical specimens, given the 200-μm resolution used in the current study. Using the stated material properties from the manufacturer in Table 1 as a starting point, a proprietary formula based on porosity was applied uniformly to the modulus, yield, and ultimate strength of each foam grade. In general, we do not scale material density (i.e., mass) in Alfonso.

Notes on the particle-based methods in *Alfonso*

- "Resolution" (e.g., 50, 200, 500 μm) in *Alfonso* is typically equivalent to the diameter of the particles in the model, and thereby the minimum distance within which particles begin to interact. The degree of interaction between particles varies continuously as a function of their distance (e.g., in compression, particles repel more vigorously the closer they are to one another, while the reverse is true for tensile forces acting between "bonded" particles of the same object).
- Each particle represents a small volume of mass of an object in the analysis, the material properties of which (elastic modulus, yield, failure, hardening criteria, etc.) dictate the responses of particles to forces applied during analysis.
- While the initial positions of particles are typically spaced in discrete increments of the resolution (e.g., 200 μm), during analysis particles may continuously move in 3D space. For instance, a particle initially at (200, 200, 200) may move to (200.0034, 199.793403, 202.09809823462) during analysis.
- "Bonds" between particles in *Alfonso* are typically formed only at the initial time state and only between neighboring particles of the same object. Bonded particles resist both compression and tension, per the homogeneous or heterogenous properties of the material, until the stress or strain failure limits of the material are exceeded, and a crack is formed. Failed particles remain in analysis (e.g., as debris) and continue to interact with other particles, allowing phenomena such as compaction to be faithfully reproduced in *Alfonso*.
- "Unbonded" particles that come into contact after analysis has begun (i.e., particles that move to within the minimum distance of interaction) will not form bonds and will only repel one another.
- (See "Beyond FEA: Particle-based simulation 101" at https://www.lifespans.net/publications for further discussion of the basics of mesh-free analysis).

Table 1. Description of Various PU Foam Grades from the Manufacturer's Datasheet and Reported Material Properties based on ASTM D1621 Compressive Tests

Foam grade	Dimensions (mm)	Density (kg/m^3)	Volume Fraction	Porosity Percentage	Manufacturer's REF number (original block)	Compressive (based on ASTM D1621)		Speed of sound $\mathbf{c}$ (m/s)
						Strength (MPa)	Modulus (MPa)	
10 PCF	10x10x10	160	0.14	86%	1522-01	2.2	58	733
15 PCF	10x10x10	240	0.20	80%	1522-02	4.9	123	871
20 PCF	10x10x10	320	0.27	73%	1522-03	8.4	210	986
40 PCF	10x10x10	640	0.46	54%	1522-05	31.0	759	1326

Uniaxial compression of physical and simulated polyurethane foam specimens

Physical foam cubes were uniaxially compressed to 10 - 15% of their original height (i.e., 1 – 1.5 mm) at a rate of 2.5 mm/min according to ASTM D1261 using an MTS 858 Mini Bionix hydraulic press (Figure 1), while recording force with a 10 kN loadcell.

Simulated foam cubes were compressed to 10% at an accelerated loading rate of 1 m/s. The speed of sound c of each foam grade was calculated to set a theoretical upper bound of rate of motion (Table 1):

$$c = \sqrt{\frac{(K_f + \frac{4}{3}G_f)}{\rho}}$$

Where for each foam grade, K_f is the bulk modulus, G_f is the shear modulus, and ρ is the density (kg/m^3) of the material. A sensitivity analysis was also conducted to confirm the maximum practical

compression rate of the simulated foam (1 m/s), below which there was no observable change in the force-displacement curve.

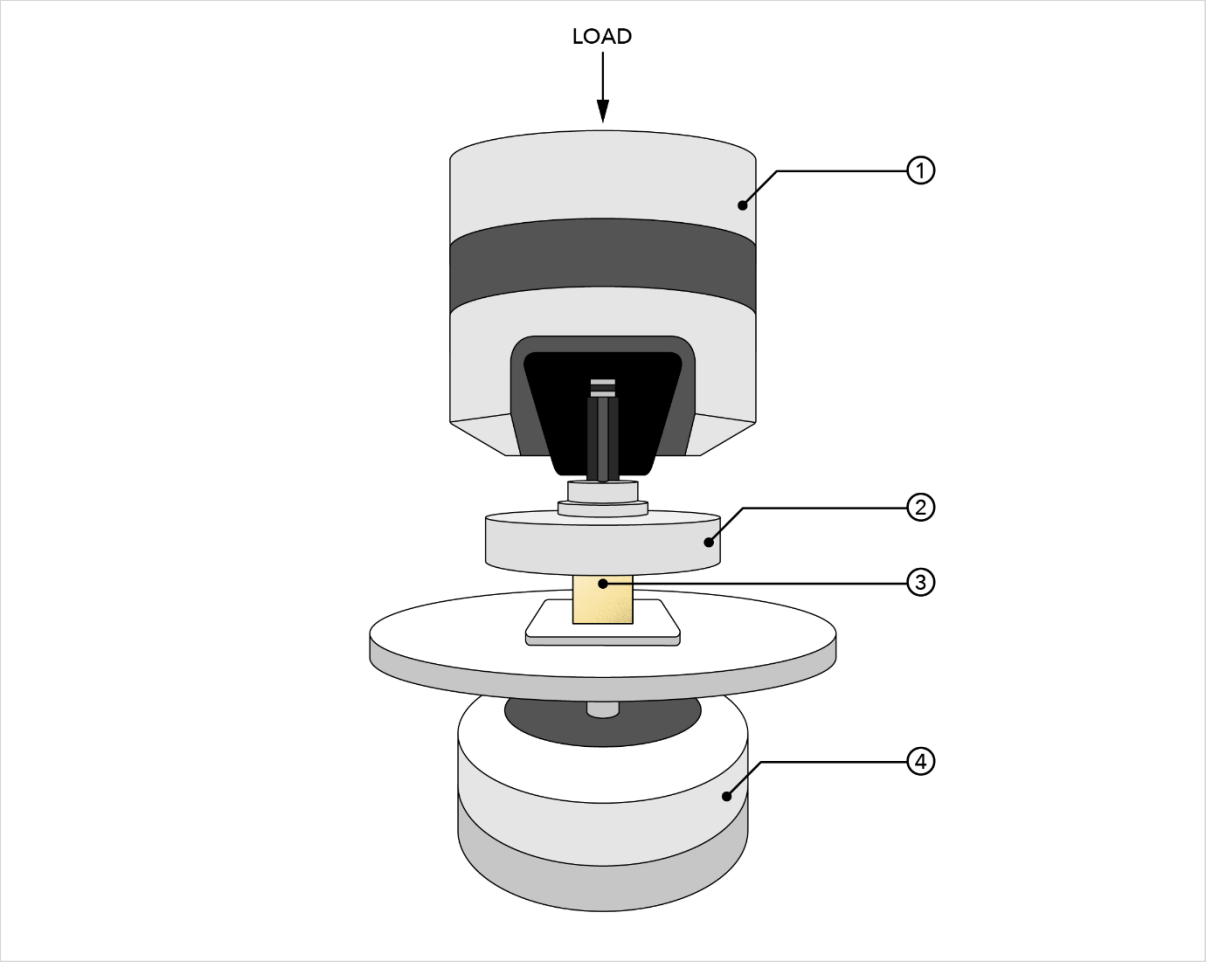

Figure 1. Physical experimental setup: 1. MTS 858 Mini Bionix hydraulic press, 2. Polished stainless steel platen, 3. Solid rigid PU foam cube (10x10x10 mm), 4. Load cell (10 kN). Illustration by Eka Tjong

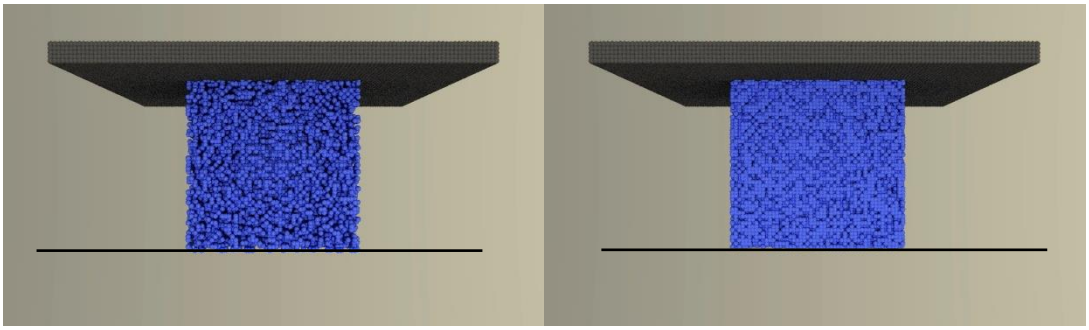

Figure 2. Simulated 10 PCF (left) and 40 PCF (right) foam, with ground planes shown as solid black lines

Data and statistical analyses

From the n = 6 physical trials of each foam grade, averages of load and displacement values were computed. The load–displacement data were normalized such that zero displacement was set at the lowest initial force common for both the physical data and the *Alfonso* simulation data.

The numbers of data points obtained from the physical tests and *Alfonso* simulations varied due to the difference in data collection intervals. In order to directly compare and analyse the load–displacement data, first a Python module package was used to resample the data sets to the same displacement values and interpolate the load values without changing the load–displacement curves' shape and magnitude. Statistical analyses were performed using an appropriate software such as MedCalc® (MedCalc Software Ltd, Ostend, Belgium).

Lin's concordance correlation coefficient (CCC)

The Lin's concordance correlation coefficient (CCC) evaluates the degree to which pairs of observations fall on the 45° line through the origin (i.e., the line of equality).[1,2][7], [8] The concordance correlation coefficient is calculated as $\rho_c = \rho \times C_b$ ($-1 \leq \rho_c \leq 1$) where:

- ρ is the Pearson correlation coefficient, which measures how far each observation deviates from the best-fit line, and is a measure of precision, and
- C_b is a bias correction factor that measures how far the best-fit line deviates from the 45° line through the origin, and is a measure of accuracy ($0 < C_b \leq 1$; $C_b = 1$ when there is no deviation from the 45° line).

A CCC value near +1 indicates strong concordance, a value near –1 indicates strong discordance, and a value near zero indicates no concordance. There is no standard for how to interpret other values, although one approach is to interpret Lin's CCC as you would for Pearson's correlation coefficient or intraclass correlation coefficients, such that values less than 0.20 have "poor" concordance, while values greater than 0.80 have "excellent" concordance.

Results

Upon the compression test, either physical or simulated, the PU foam was crushed. The generated load-displacement curves as shown in Figure 6 during this foam compression generally have linear-elastic behaviors in loading up to the material failure (e.g., fracture). Both the physical and simulated curves have the typical three distinct regions corresponding to the behaviors of the PU foam's cell walls during compression [9]. Firstly, the linear elastic phase up to 1 mm of the displacement where the cell walls in the PU foam started to bend due to the small increases of loads. Secondly, the long plateau collapse phase that occupied the majority of the load-displacement curve where the cell walls buckled, yielded, or fractured. Lastly, towards the end of the load-displacement curve, the densification phase was displayed as the cell walls eventually compacted and crushed together. Quantitative analyses in Table 2 shows that the concordance between the physical and simulated compression tests across different PU foam grades are all well above 0.85.

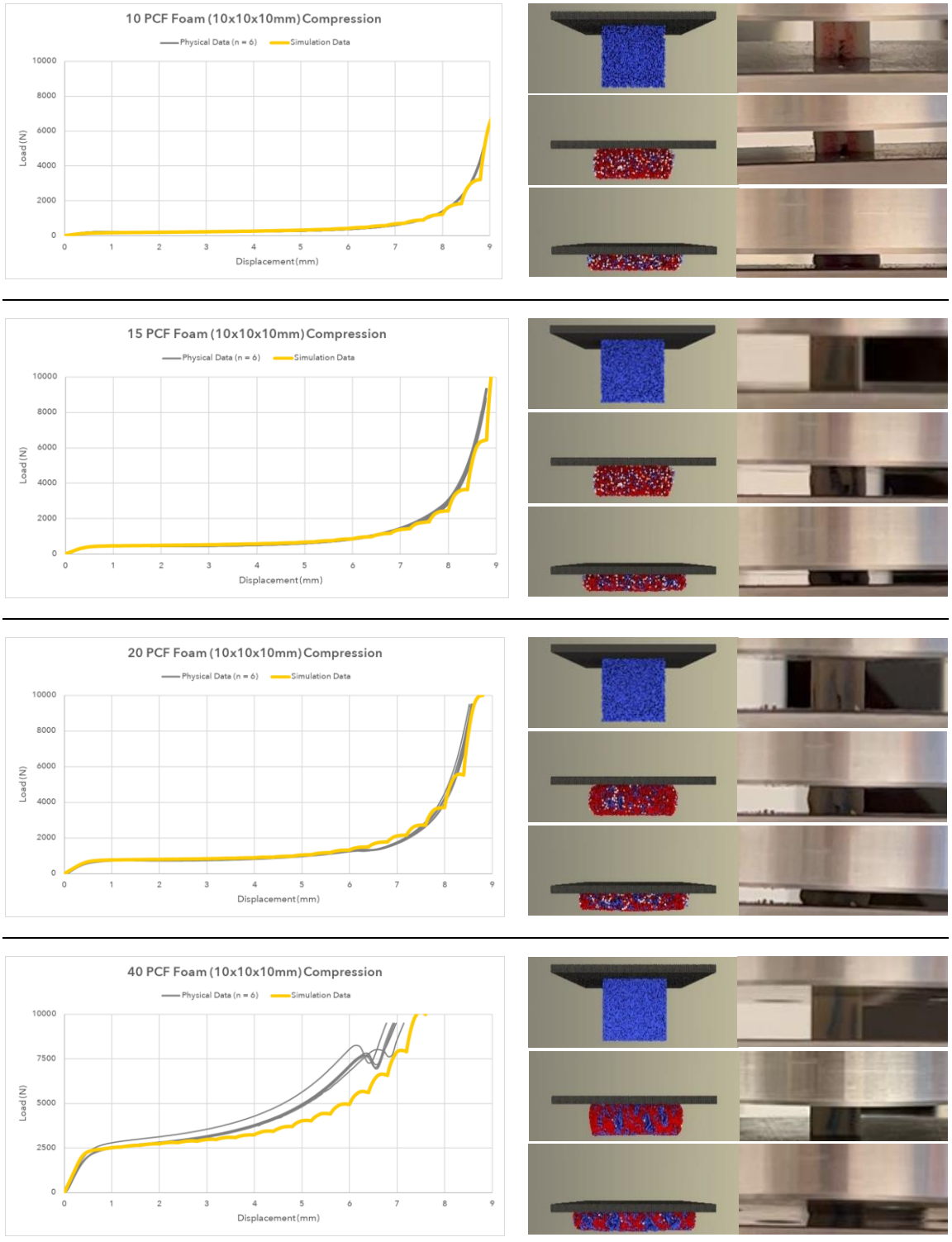

Figure 3. Force-displacement curves and images of simulated and physical compression tests of (from top) 10, 15, 20, and 40 PCF PU 10 mm foam cubes to 10-15% of their original height

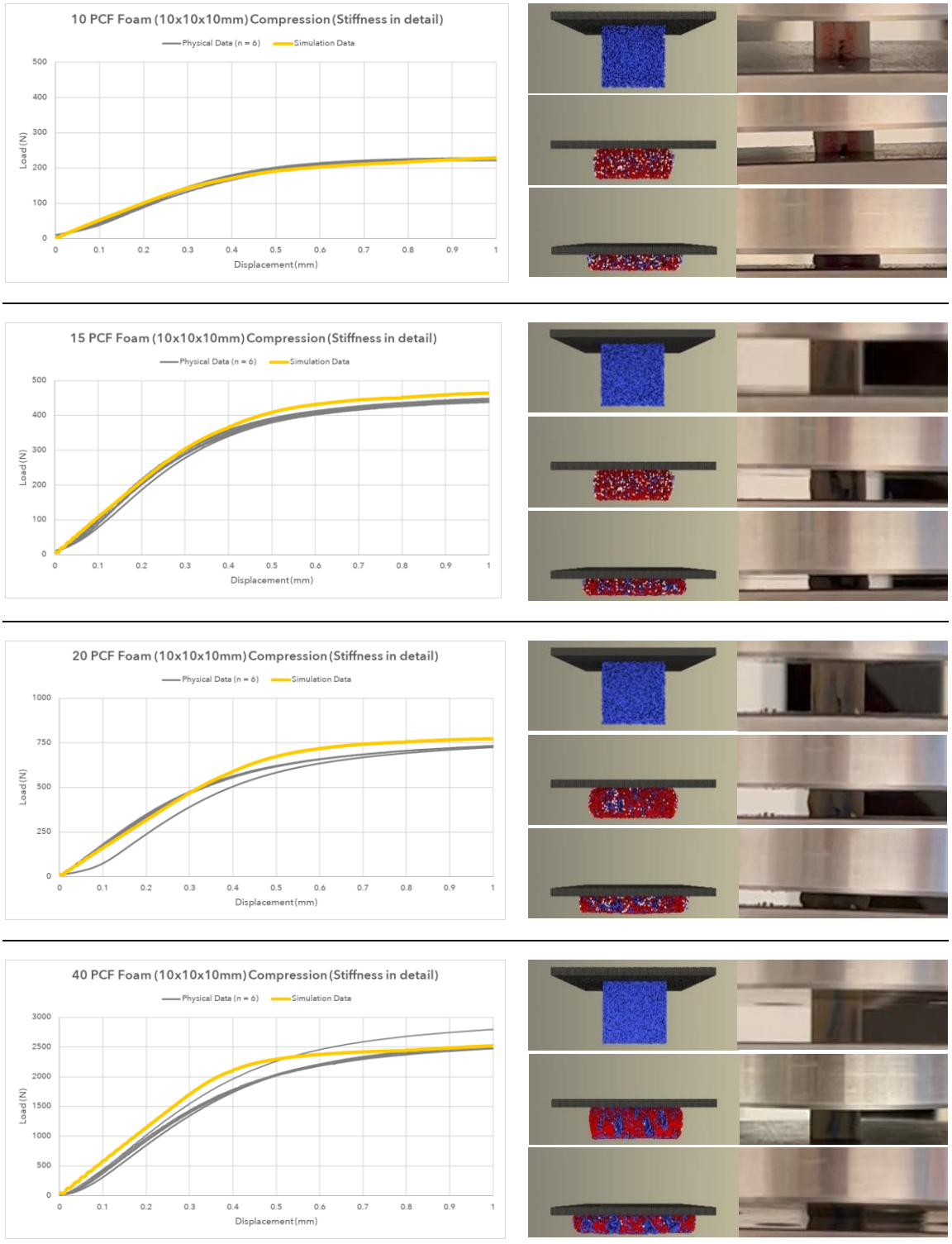

Figure 4. Force-displacement curves (focused on stiffness slopes) and images of simulated and physical compression tests of (from top) 10, 15, 20, and 40 PCF PU 10 mm foam cubes to 10-15% of their original height

Table 2. Concordance analysis on physical versus simulated foam compression tests on various PU foam grades

Variables	Average Physical Trials (n = 6) vs Simulation			
	10 PCF	15 PCF	20 PCF	40 PCF
Sample size (curve data points)	442	442	430	348
Concordance correlation coefficient	0.9909	0.9909	0.9883	0.8714
95% Confidence Interval	0.9895 to 0.9920	0.9895 to 0.9920	0.9860 to 0.9902	0.8542 to 0.8868
Pearson ρ (precision)	0.995	0.995	0.9924	0.9801
Bias correction factor C_b (accuracy)	0.9958	0.9958	0.9958	0.8891

Conclusion

The concordance correlation coefficient between the force-displacement curves of experimental and simulated pairs was 0.99, 0.99, 0.98, and 0.87 for 10, 15, 20, and 40 PCF foam, respectively. Experimental and simulated pairs likewise produced similar qualitative patterns of damage during compression. Alfonso under-estimated the force during the densification phase of the 40 PCF foam compression, most likely due to the coarse granularity of the simulated foam debris particles relative to the physical case; finer resolution modelling may improve convergence.

Alfonso can generate accurate models of solid rigid polyurethane foam compression and failure, especially for low and medium-density foam grades.

References

[1] P. S. D. Patel, D. E. T. Shepherd, and D. W. L. Hukins, "Compressive properties of commercially available polyurethane foams as mechanical models for osteoporotic human cancellous bone," *BMC Musculoskelet Disord*, vol. 9, no. 137, 2008, doi: 10.1186/1471-2474-9-137.

[2] J. A. Svizek, J. D. Thompson, and J. B. Benjamin, "Characterization of Three Formulations of a Synthetic Foam as Models for a Range of Human Cancellous Bone Types," *Journal of Applied Biomaterials*, vol. 6, pp. 125–128, 1995.

[3] K. L. Calvert, K. P. Trumble, T. J. Webster, and L. A. Kirkpatrick, "Characterization of commercial rigid polyurethane foams used as bone analogs for implant testing," *J Mater Sci Mater Med*, vol. 21, no. 5, pp. 1453–1461, May 2010, doi: 10.1007/s10856-010-4024-6.

[4] V. Palissery, M. Taylor, and M. Browne, "Fatigue characterization of a polymer foam to use as a cancellous bone analog material in the assessment of orthopaedic devices," *J Mater Sci Mater Med*, vol. 15, pp. 61–67, 2004.

[5] J. D. Rehkopf, G. M. McNeice, and G. W. Broadland, "Fluid and Matrix Components of Polyurethane Foam Behavior Under Cyclic Compression," *ASME*, vol. 118, pp. 58–62, 1996, [Online]. Available: http://materialstechnology.asmedigitalcollection.asme.org/pdfaccess.ashx?url=/data/journals/jemta8/26976/

[6] A. J. C. Ladd and J. H. Kinney, "Numerical errors and uncertainties in finite-element modeling of trabecular bone," 1998.

[7] L. I.-K. Lin, "A Concordance Correlation Coefficient to Evaluate Reproducibility," *Biometrics*, vol. 45, no. 1, p. 255, Mar. 1989, doi: 10.2307/2532051.

[8] MedCalc Software Ltd, "Concordance correlation coefficient." https://www.medcalc.org/manual/concordance.php (accessed May 27, 2022).

[9] J. v. Mane *et al.*, "Mechanical Property Evaluation of Polyurethane Foam under Quasi-static and Dynamic Strain Rates- An Experimental Study," in *Procedia Engineering*, 2017, vol. 173, pp. 726–731. doi: 10.1016/j.proeng.2016.12.160.